Histol Histopathol (2009) 24: 187-196

http://www.hh.um.es

Histology and Histopathology

Cellular and Molecular Biology

Distribution of cytoskeletal and adhesion proteins in adult zebrafish skeletal muscle

E.S. Câmara-Pereira[1,2,*], L.M. Campos[1,2,*], M.A. Vannier-Santos[2], C.S. Mermelstein[1] and M.L. Costa[1]

[1]Instituto de Ciências Biomédicas, Universidade Federal do Rio de Janeiro, Rio de Janeiro, RJ, Brazil and

[2]Centro de Pesquisas Gonçalo Moniz, Fundação Oswaldo Cruz, Salvador, Bahia, Brazil

* E.S.C.P. and L.M.C. contributed equally to this work

Summary. The organization of cytoskeletal and adhesion proteins in skeletal muscle is critical for its contractile function. Zebrafish has become a paramount model for studies of vertebrate biology, including muscle. However, only a few studies have been published using immunolabeling to specifically localize proteins in adult zebrafish muscle. To fully appreciate the distribution of cytoskeletal and adhesion proteins, and therefore to better correlate the adult muscle with its myogenesis, we used indirect immunofluorescence microscopy of frozen adult zebrafish skeletal muscle sections. Here we describe the fish muscle cytoskeletal architecture and location of the major myofibrillar proteins desmin, alpha-actinin, myosin, titin, troponin, tropomyosin and nebulin, the adhesion proteins vinculin and paxillin, and the extracellular matrix proteins laminin and fibronectin. Electron microscopical analysis in ultra-thin sections of adult zebrafish skeletal muscle showed bundles of collagen fibers and fibroblastic cells in the extracellular space of the myosepta.

Key words: Muscle, Zebrafish, Cytoskeleton, Extracellular matrix, Cell adhesion

Introduction

The contractile function of skeletal muscle is based on its particular arrangement of cytoskeletal and adhesion proteins. To understand muscle function, one needs to understand each of its component molecules, their relationship and its overall architecture. Several animal models have been studied to understand muscle architecture, including mammals, avian, fishes and flies. Among these models, the freshwater zebrafish (*Danio rerio*) has been vastly studied as a model organism for studies of vertebrate biology. Zebrafish has the advantage of external development with optically transparent embryos, a large number of offspring (50-350 per week) and rapid development. Recent studies have indicated that the zebrafish can be used as a model for human diseases (Zon, 1999), such as muscular dystrophies (Bassett and Currie, 2003). The majority of the studies with zebrafish muscle have been made in embryos, due to the above-cited advantages of studying its development. Nevertheless, it is also important to know how the adult zebrafish muscle is organized. Skeletal muscle of adult zebrafish has been structurally studied before (Waterman, 1969; van Raamsdonk et al., 1982), but there was no characterization of muscle proteins. The muscle fiber diversity and anatomical organization of the myotomes of developing zebrafish embryos and larvae are much simpler than those of the adult. Only two fiber types are present in the embryos: embryonic slow red muscle and embryonic fast white muscle (Waterman, 1969; van Raamsdonk et al., 1982). This contrasts with the five fiber types found in the adult (van Raamsdonk et al., 1982, 1987). Moreover, only a few studies have been published using immunolabeling to specifically localize proteins in adult zebrafish muscle (Chambers et al., 2001; Guyon et al., 2005). In the present work, we studied the overall muscle cytoskeletal architecture and the distribution of the main cytoskeletal, sarcomeric, adhesion and extracellular matrix proteins in adult zebrafish skeletal muscle. It is the first description of the organization of these proteins in mature muscle fibers of the fish using immunofluorescence microscopy. Furthermore, using transmission electron microscopy of the adult fish skeletal muscle we performed an ultrastructural analysis of myofibrils, sarcoplasmic reticulum, mitochondria and components of the myoseptal region.

Offprint requests to: Dr. Manoel Luis Costa, Instituto de Ciências Biomédicas, Universidade Federal do Rio de Janeiro, Rio de Janeiro, RJ, 21949-590, Brazil. e-mail: manoelluiscosta@ufrj.br

Materials and methods

Antibodies and fluorescent probes

DNA-binding probe DAPI (4,6-Diamidino-2-phenylindole dyhydrochloride) was purchased from Molecular Probes (Invitrogen, São Paulo, Brasil). The following primary antibodies were all purchased from Sigma Chemical Co. (St. Louis, MO, USA): mouse monoclonal anti-sarcomeric alpha-actinin (A-7811), mouse monoclonal anti-collagen IV (C-1926), rabbit polyclonal anti-desmin (D-8281), rabbit polyclonal anti-fibronectin (F-3648), rabbit polyclonal anti-laminin (L-9393), rabbit polyclonal anti-skeletal myosin (M-7523), mouse monoclonal anti-skeletal myosin fast (M-4276), mouse monoclonal anti-skeletal myosin slow (M-8421), mouse monoclonal anti-nebulin (N-9891), mouse monoclonal anti-troponin T (T-6277), mouse monoclonal anti-titin T11 (T-9030), mouse monoclonal anti-sarcomeric tropomyosin (T-9283), mouse monoclonal anti-vinculin (V-4505). Mouse monoclonal anti-paxillin antibody (code 610619) was purchased from BD Transduction Laboratories (San Jose, CA, USA). Fluorescein isothiocyanate (FITC)-goat anti-mouse/rabbit IgG and tetramethylrhodamine isothiocyanate (TRITC)-goat anti-mouse/rabbit IgG antibodies were purchased from Sigma.

Zebrafish maintenance

Adult wild-type zebrafish (*Danio rerio*) were kept in a 14 hour light cycle in system water at 28°C, according to standard procedures (Westerfield, 2000). We developed our own zebrafish aquarium system, with several independent 7-liter tanks and central water processing, with mechanical (glass wool), chemical (activated carbon) and biological (porous ceramic) filters. Temperature was controlled by air-conditioning and water heater. National Research Council guidelines were followed.

Fixation and cryosectioning of zebrafish specimens

Specimens of adult zebrafish were anesthetized by lowering the temperature to -20°C for 15 minutes, killed by decapitation, and then fixed in 4% paraformaldehyde in phosphate buffer saline (PBS, pH 7.4) for 5 minutes. After fixation, specimens were incubated with 30% sacarose for 2 hours, attached to a wood stick using Tissue Tek Compound, and frozen in isopentane previously kept in liquid nitrogen. Longitudinal and transverse sections of 10 µm were obtained in a Leica Cryostat (model CM1850, Leica, Wetzlar, Germany), placed in poly-L-lysine-coated slides and kept at -70°C.

Autofluorescence elimination

Two different chemicals were tested in order to eliminate autofluorescence: ammonium chloride (NH_4Cl) and sodium borohydride (Borax, $NaBH_4$). We used the three following conditions:
1- incubation with PBS for 1 hour (control condition);
2 - incubation with 2% Borax for 1 hour;
3 - incubation with 50 mM NH_4Cl for 1 hour.

To determine more precisely the emission spectrum of the autofluorescence, sections of zebrafish muscle were analyzed in a LSM510 Meta Scanning Confocal Microscope (Zeiss, Oberkochen, Germany). The lambda scans were performed using a 488/560 dichroic mirror, and argon-kripton laser.

Immunofluorescence microscopy and imaging

Zebrafish frozen sections were permeabilized twice with 0.25% Triton X-100 in PBS for 10 minutes each. Specimens were blocked for autofluorescence with 50 mM NH_4Cl for 1 hour and then washed twice with PBS for 5 minutes each. Non-specific binding of antibodies was blocked by incubation of frozen sections for 24 hours at 4°C with 2.5% bovine serum albumin, 8% fetal bovine serum and 2% skimmed milk in PBS. Specimens were then washed twice with 0.25% Triton X-100 in PBS (PBS-T) for 5 minutes each, and incubated with primary antibodies, at appropriate dilutions, for 1 h at 37°C in a humid chamber. After incubation, they were washed three times for 10 minutes in PBS-T and incubated with TRITC-labeled secondary antibodies for 1 hour at 37°C in a humid chamber. After a 30 minutes wash with PBS-T, DAPI (0.1 µg/ml in 0.9% NaCl) was added for 5 minutes. Then, they were washed for 3 minutes with 0.9% NaCl and mounted in glass slides with glycerol containing (w/v) 5% n-propyl gallate, 0.25% 1,4-diazabi-cyclo(2,2,2)octane (DABCO) and 0.0025% para-phenylenediamine (all from Sigma). The stained sections were visualized in a Zeiss Axiovert 100 inverted microscope (Carl Zeiss, Oberkochen, Germany) using appropriate filters for fluorescence and DIC. For image acquisition, analog video enhancement and digital background subtraction, we used an integrated Hamamatsu CCD camera (Hamamatsu Photonics, Shizuoka, Japan), with a Hamamatsu Argus 20 image processor and a Dell GL75 computer (Dell Corporate, Round Rock, TX, USA). Some images were acquired with a LSM510 Zeiss confocal microscope, in separated steps to minimize cross talk between the channels. Images were processed with the ImageJ software, based on the public domain NIH Image program (developed at the U.S. National Institutes of Health and available on the Internet at http://rsb.info.nih.gov/nih-image/). Plates were mounted using Adobe Photoshop (Adobe Systems Incorporated, San Jose, CA, USA). Control experiments with no primary antibodies showed only faint background staining (data not shown).

Transmission electron microscopy (TEM)

Fragments (*circa* 1 mm^3) of adult zebrafish skeletal muscle were processed for TEM as described below. They were placed in a vial of fixative solution containing 4% paraformaldehyde, 4% glutaraldehyde in

0.1 M sodium cacodilate buffer pH 7.4 for 1 hour at 4°C. The samples were rinsed 3 times for 10 minutes in 0.1 M sodium cacodilate buffer, post-fixed in 1% osmium tetroxide in the same buffer for 1 hour at 4°C, dehydrated in a graded series of acetone solutions (30%, 50%, 70%, 95%, 100%), and embedded in Polybed resin (Electron Microscopy Sciences, USA). Transverse and longitudinal ultra-thin sections (80 nm-thick) were obtained with an ultramicrotome (model CM1850, Leica, Wetzlar, Germany) with a diamond knife (Diatome AG, Biel, Switzerland), deposited on copper grids (400 mesh), and stained with 2% uranyl acetate for 20 minutes and 1% lead citrate for 5 minutes. The ultra-thin sections were observed in a Jeol 1200 EX electron microscope (Jeol, Tokyo, Japan), operated at 80 kV.

Results

Prior to studying the distribution of the main cytoskeletal, sarcomeric, adhesion and extracellular matrix proteins in adult zebrafish skeletal muscle, we wanted to ensure that the immunofluorescence label of these proteins could be specifically detected without any interfering non-specific fluorescence. Fixed frozen sections of adult zebrafish skeletal muscle (with no antibody incubation) were analyzed under a conventional inverted fluorescence microscope. A high level of green autofluorescence (450-490 nm) was observed (data not shown), as well as a lower level of red (546 nm) and UV autofluorescence (365 nm). It has been reported that some tissues have high levels of autofluorescence which can confound analysis (Jackson et al., 2004). One of such tissues is the striated skeletal muscle. Thus, in an attempt to reduce the observed autofluorescence in zebrafish muscle, we tested two different chemicals that have been described as being effective in autofluorescence elimination: ammonium chloride and sodium borohydride. Only the ammonium chloride (50 mM) was effective in the elimination of autofluorescence in the 546 nm (red) and in the 365 nm (UV) fluorescence channels. None of the chemicals (50 mM ammonium chloride and 2% sodium borohydride) were able to eliminate the autofluorescence in the 450-490 nm (green) fluorescence channel. To better characterize the correction of autofluorescence, we examined the tissue samples using a spectral confocal microscope (Fig. 1). Employing the conditions used for fluoresceine isothiocyanate (FITC) and tetramethyl-

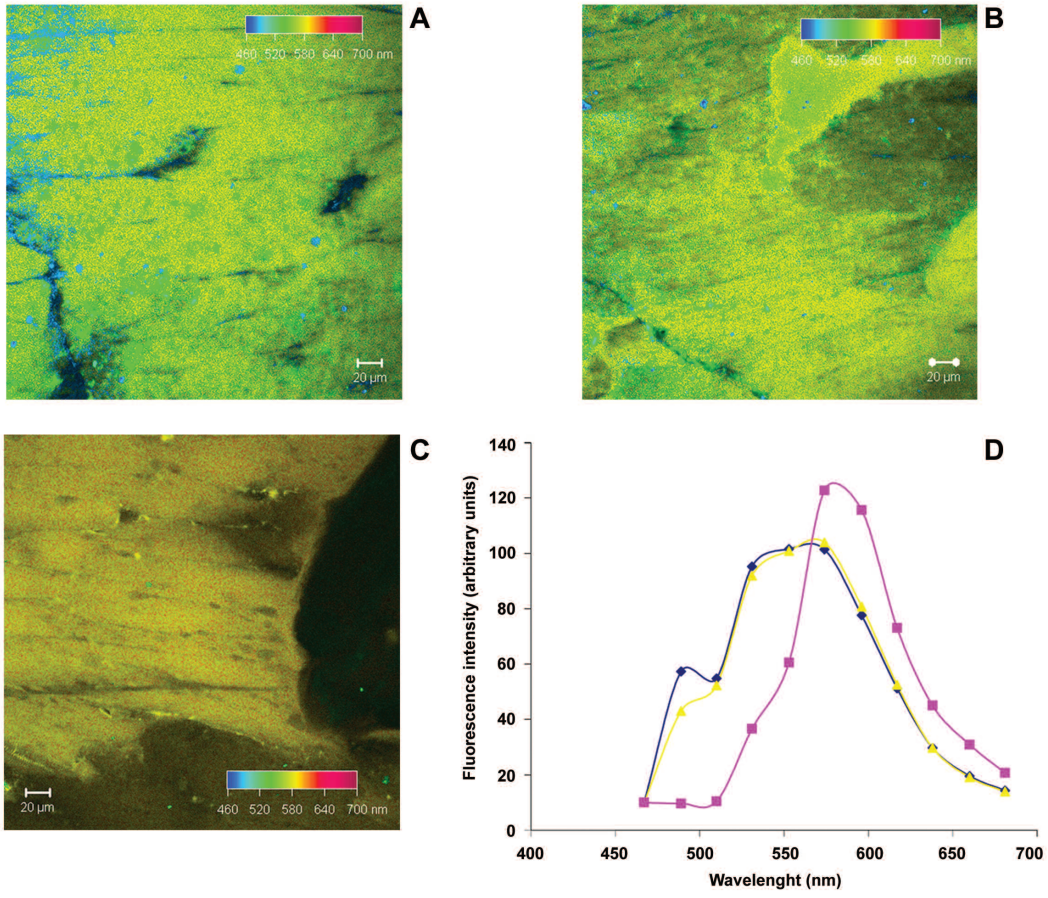

Fig. 1. Autofluorescence in adult zebrafish skeletal muscle. Skeletal muscle tissue samples were analyzed under spectral confocal microscopy. Emission in several wavelengths (from 460-700 nm) was scanned. Note that the fluorescence emission is higher at about 550 nm for both unlabeled (**A and D**, blue line) and primary and FITC-secondary labeled sections (**B and D**, yellow line), while it is higher at about 590 nm for primary and TRITC-secondary labeled sections (**C and D**, pink line). The FITC-immunolabel (**B and D**) does not differ from autofluorescence alone (**A and D**), while TRITC-label is quite different from the control condition (**C and D**). Colors in A-C correspond to the maximal wavelength of the lambda scan. Scale bars: 20 µm.

rhodamine isothiocyanate (TRITC) studies, we scanned the emission in several wavelengths (from 460-700 nm). We could see that the fluorescence emission was higher at about 550 nm for both unlabeled (Fig. 1A) and primary and FITC-secondary labeled (Fig. 1B) sections, while it was higher at about 590 nm for primary and TRITC-secondary labeled sections (Fig. 1C). Therefore, the FITC-immunolabel does not differ from autofluorescence alone, while TRITC-label is quite different from the control condition (Fig. 1D). This result can be seen in Figs. 1A-C, where the colors correspond to the maximal wavelength of the lambda scan stack.

We then established the following protocol for all the subsequent immunofluorescence stainings of frozen sections of zebrafish muscle: 1) incubation with 0.25%

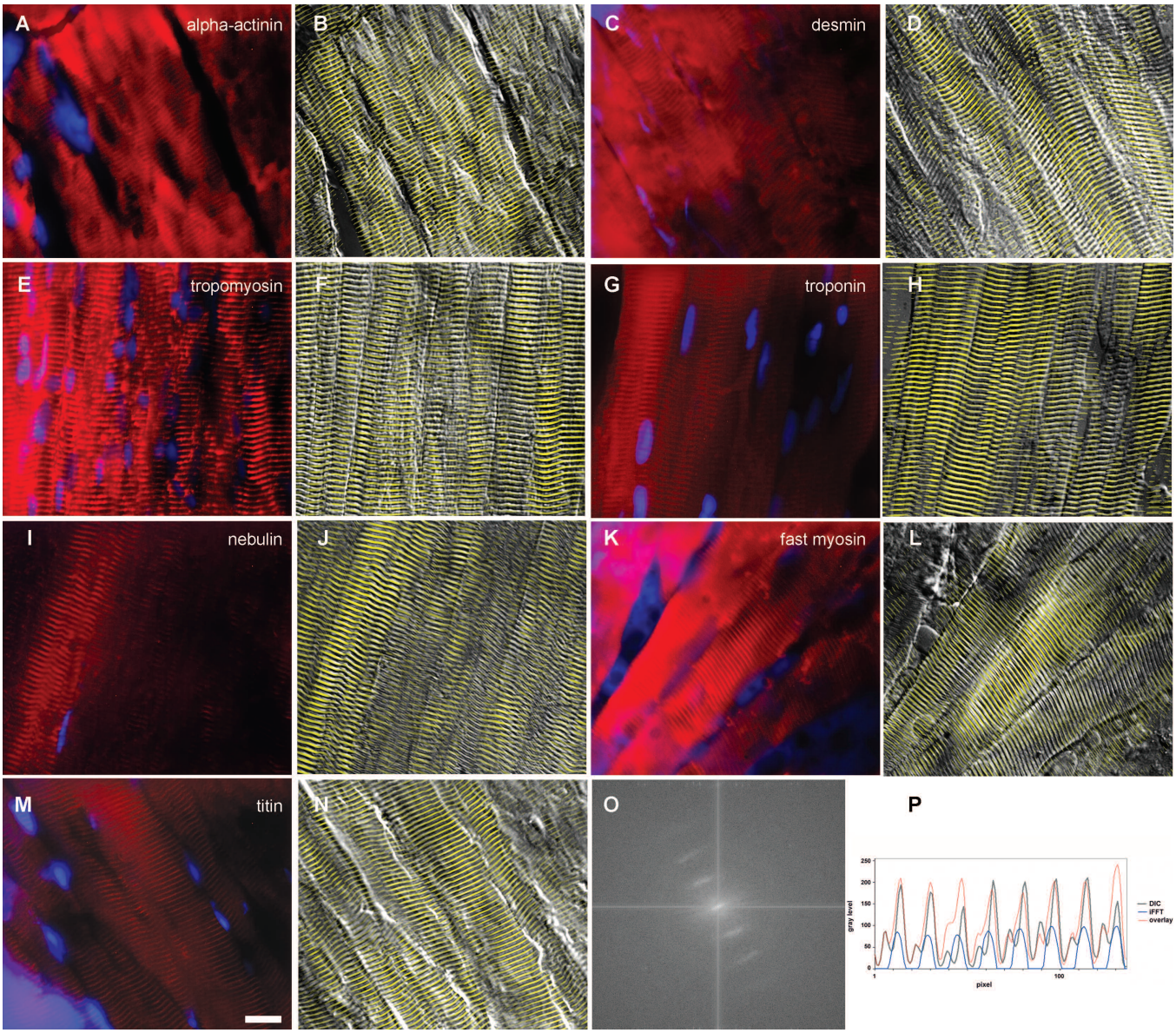

Fig. 2. Immunolocalization of sarcomeric proteins in adult zebrafish skeletal muscle. Frozen skeletal muscle longitudinal sections were stained with antibodies against the following cytoskeletal proteins: sarcomeric alpha-actinin (**A, B**), desmin (**C, D**), tropomyosin (**E, F**), troponin T (**G, H**), nebulin (**I, J**), skeletal myosin fast (**K, L**) and titin (**M, N**). Secondary antibodies labeled only with TRITC were used. The antibody stain (red) is compared to the nuclei stain (blue, **A, C, E, G, I, K, M**). The same field was visualized with DIC optics (gray, **B, D, F, H, J, L, N**). These images were overlaid with the inverse transform of selected Fast Fourier transform regions, shown in yellow (**B, D, F, H, J, L, N**). Typical Fast Fourier transform of sarcomeric protein stain (tropomyosin, **O**); images such as this were used to enhance periodic features and generate the inverse transforms. To show the periodicity of the stains and their comparison to the DIC image, we did a densitometry across several sarcomeres (**P**): in blue, intensities along the line pointed by an arrow in image **F** of the inverse transform; in grey, intensities along the DIC image; and in red, the sum of both lines. Scale bar: 20 μm.

Triton X-100 (to permeabilize the muscle fragments); 2) pre-incubation with 50 mM ammonium chloride (to block autofluorescence); 3) incubation with 2.5% bovine serum albumin, 8% fetal bovine serum and 2% skimmed milk (to block non-specific binding of antibodies); 4) incubation with primary antibodies; 5) incubation with TRITC-goat anti-mouse/rabbit IgG antibodies.

We next analyzed by immunofluorescence microscopy the distribution of several sarcomeric proteins in frozen longitudinal sections of adult zebrafish muscle (Fig. 2) and confirmed their periodic display: the Z-line alpha-actinin (Fig. 2A,B), the intermediate filament desmin (Fig. 2C,D), the I-band tropomyosin (Fig. 2E,F), the I-band troponin (Fig. 2G,H), the I-band nebulin (Figs. 2I,J), and the A-band myosin (Fig. 2K,L). We also analyzed titin (Fig. 2M,N), which spans the whole sarcomere. Measurements of sarcomere length in these immunofluorescence images varied from 1.7-2.0 µm.

Since the immunolabels of sarcomeric proteins

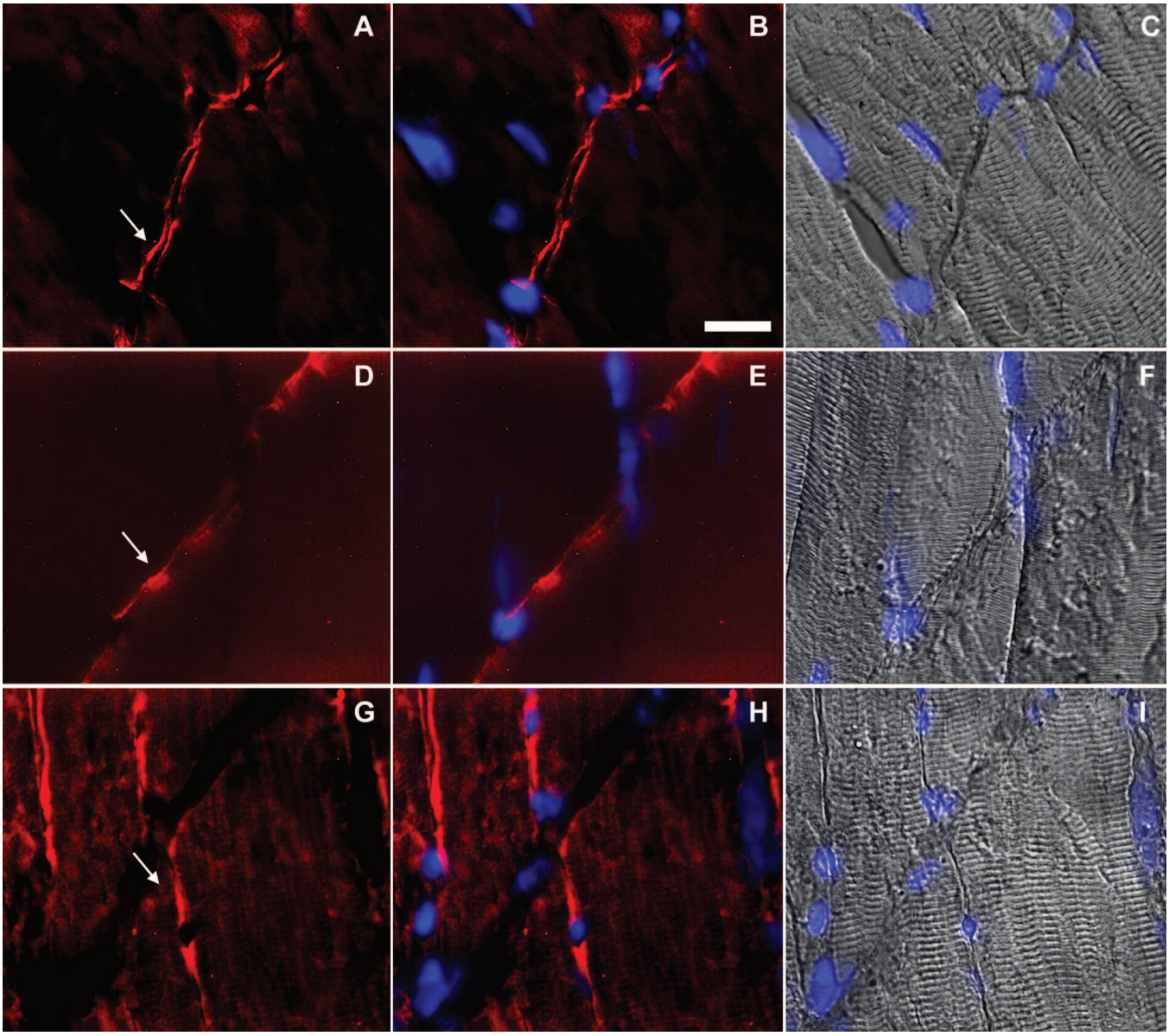

Fig. 3. Immunolocalization of adhesion proteins in adult zebrafish skeletal muscle. Frozen skeletal muscle longitudinal sections were stained with antibodies against the following proteins: paxillin (**A, B**), vinculin (**D, E**), sarcomeric alpha-actinin (**G, H**). Secondary antibodies labeled only with TRITC were used. Nuclei were stained with DAPI (**B, C, E, F, H, I**). DIC is shown in images **C, F and I**. Paxillin and vinculin are concentrated at the myoseptal region (arrows in **A and D**) and alpha-actinin is concentrated at cell-cell adhesion sites (arrow in **G**). Scale bar: 10 µm.

seemed to be periodical, we used fast Fourier transforms (FFTs) to analyze the distribution of each protein and improve the stained images (Fig. 2). We show in the FFTs that all the immunolabels have an important concentration of periodical structures within the expected sarcomere width of 1.7-2.0 µm. By selecting these structures and performing inverse FFTs, we produced images (Fig. 2, yellow) overlaid with the DIC images (Fig. 2, gray).

We also examined the distribution of adhesion proteins in the adult zebrafish muscle (Fig. 3). Paxillin (Fig. 3A,B) and vinculin (Fig. 3D,E) were found at the myoseptal region (see arrows) in continuous lines along the sarcolemma, which can be seen in the DIC images (Fig. 3C,F). Sarcomeric alpha-actinin was found in Z-lines (Fig. 2A,B) and also in cell-cell adhesion sites within the myotome (Fig. 3G-I). The nuclei stain with the fluorescent probe DAPI shows the presence of nuclei in the septa region between two myotomes (Fig. 3B,C,E,F,H,I), which could indicate the presence of fibroblastic cells. Further, we analyzed the immunolocalization of extracellular matrix proteins in frozen longitudinal sections of adult zebrafish skeletal muscle (Fig. 4). Fibronectin and laminin were found concentrated at the myoseptal region (Fig. 4A,B,D,E) in continuous lines along the sarcolemma, similar to the distribution of the adhesion proteins vinculin and paxillin (Fig. 3).

We used transmission electron microscopy (TEM) to further analyze the ultrastructure of the adult zebrafish skeletal muscle (Figs. 5-7). Parallel myofibrils are seen in longitudinal sections of the adult fish muscle (Fig. 5A,B), where they exhibit distinct Z-lines (Z), A-bands (A), I-bands (I) and M-lines (M). Cisternae of the sarcoplasmic reticulum are in close association with most of the myofibrils (Fig. 5A, arrow). The typical hexagonal arrangement (6 actin filaments around each myosin filament) of the myofilaments can be visualized in transverse sections of the adult fish muscle (Fig. 6A-C). Many mitochondria were found in close proximity to myofibrils (Fig. 7B, arrow). Bundles of collagen fibers and centrally located fibroblastic cells were seen in the extracellular space of the septa between the myotomes (Fig. 7D, arrow).

Discussion

We carried out a study on the organization of the sarcomeric proteins alpha-actinin, desmin, tropomyosin, troponin, nebulin, myosin and titin, the adhesion proteins

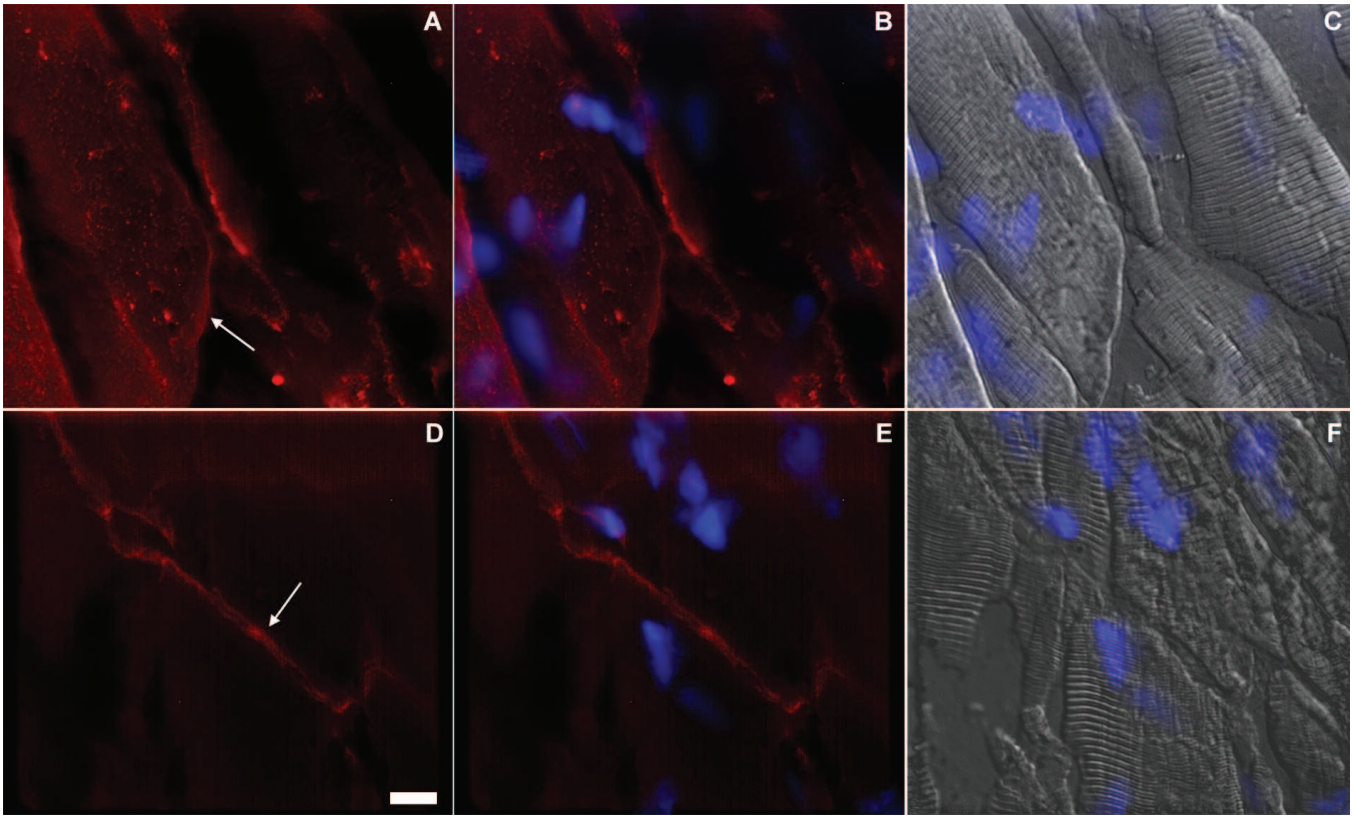

Fig. 4. Immunolocalization of extracellular matrix proteins in adult zebrafish skeletal muscle. Skeletal muscle frozen longitudinal sections were stained with antibodies against fibronectin (**A, B**) and laminin (**D, E**). Secondary antibodies labeled only with TRITC were used. Nuclei were stained with DAPI (**B, C, E, F**). DIC is shown in images **C** and **F**. Fibronectin and laminin are concentrated at the myoseptal region (arrows in **A** and **D**). Scale bar: 10 µm.

vinculin and paxillin, and the extracellular proteins fibronectin and laminin in adult zebrafish skeletal muscle using immunofluorescence microscopy. Zebrafish has recently emerged as an important model organism for the study of muscular dystrophies and other human diseases (Zon, 1999), as well as for drug and pollutant screens using whole vertebrates. However, the majority of the studies with zebrafish muscle have been done with embryos and only a few studies have been published which specifically localize proteins in adult zebrafish muscle (Chambers et al., 2001; Guyon et al., 2005). The lack of detailed analysis on the distribution of cytoskeletal, sarcomeric, adhesion and extracellular proteins in the adult zebrafish muscle may jeopardize future investigations using this animal model. In particular, some of the muscle diseases involve the

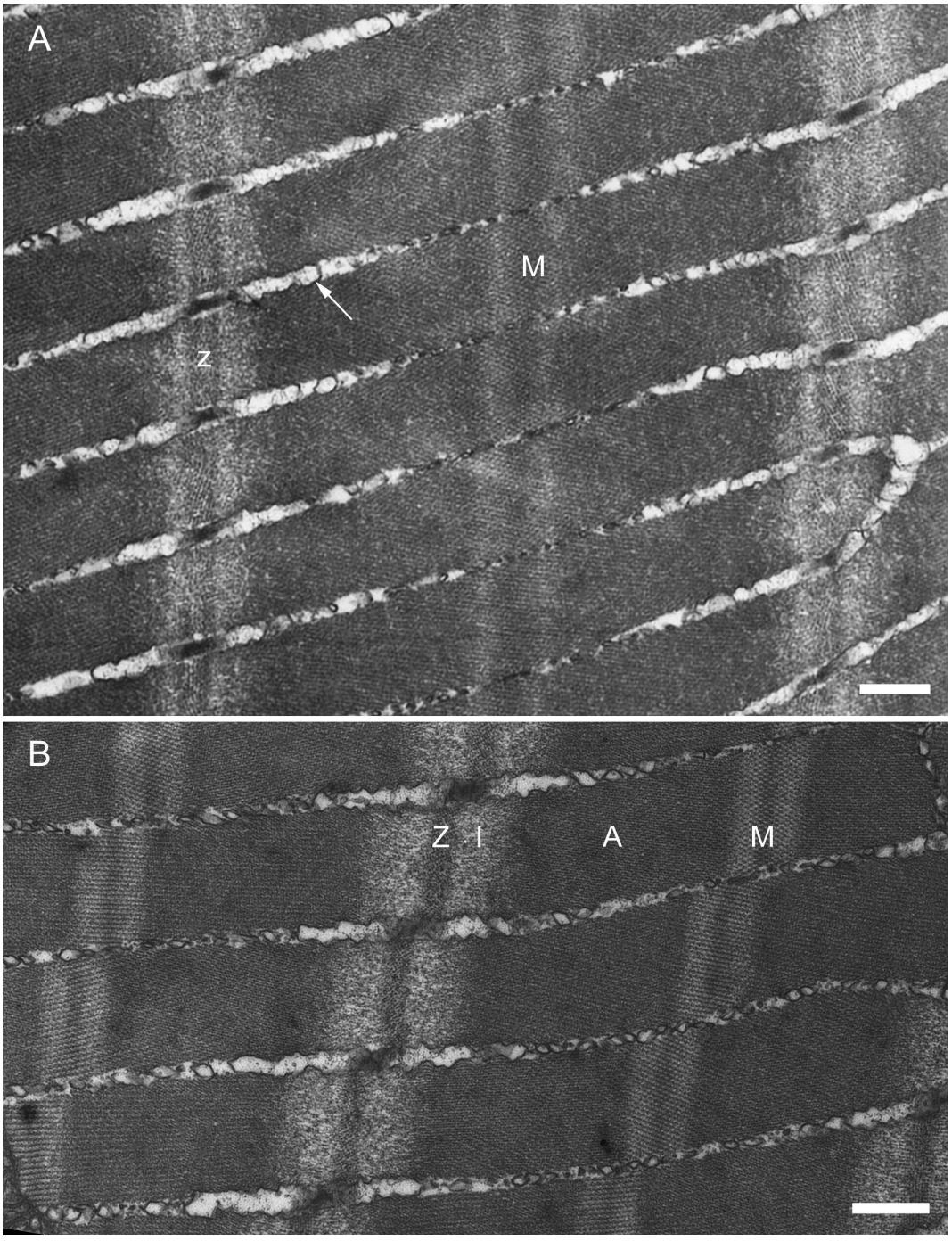

Fig. 5. Ultrastructure of myofibers in the adult zebrafish skeletal muscle. Longitudinal sections of adult zebrafish skeletal muscle processed for transmission electron microscopy shows several aligned sarcomeres (**A and B**). Cisternae of the sarcoplasmic reticulum are in close association with most of the myofibrils (arrow in A). Z: Z-line, I: I-band, A: A-band, M: M-line. Scale bars: 50 nm.

cytoskeletal and adhesion structures that we studied in this paper.

A critical point in our investigation was the high levels of autofluorescence in the adult zebrafish muscle. It has been reported that striated skeletal muscle tissues have high levels of autofluorescence that can confound analysis (Jackson et al., 2004). We found an intense autofluorescence in the range of 450-490 nm in the adult zebrafish skeletal muscle, which was abolished with a pre-incubation with 50 mM ammonium chloride. The elimination of the autofluorescence was crucial for a detailed analysis of the distribution of specific cytoskeletal and adhesion proteins in the fish muscle.

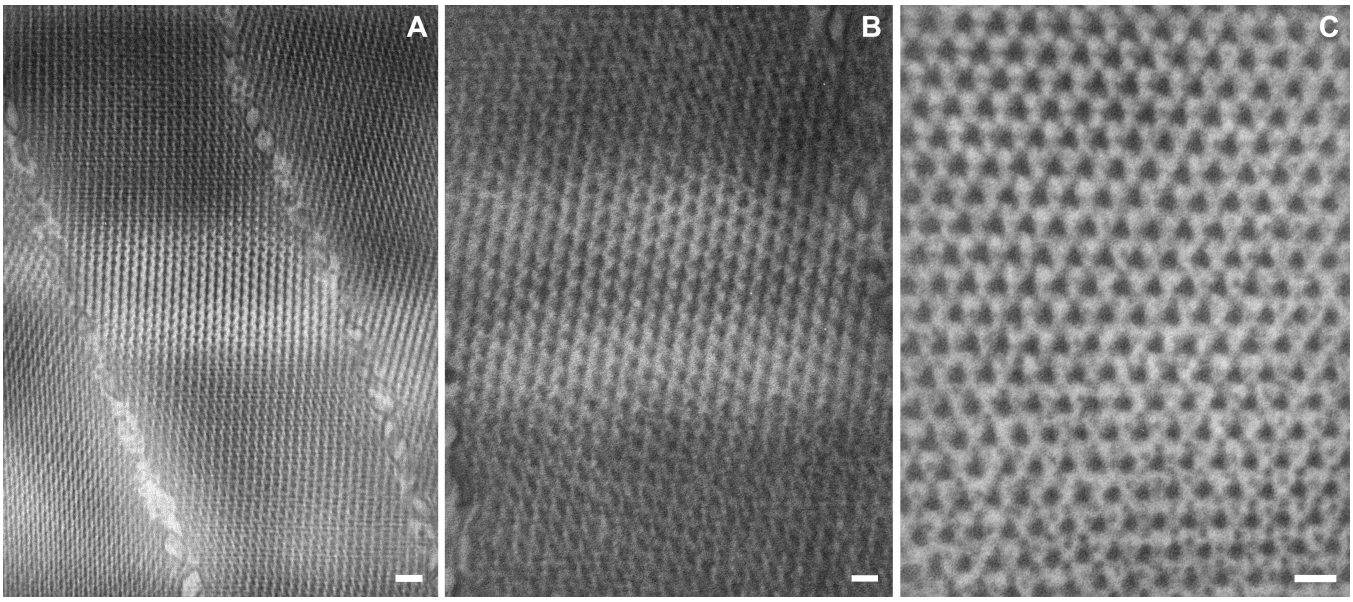

Fig. 6. Ultrastructure of myofibers in the adult zebrafish skeletal muscle. Transverse sections of adult zebrafish skeletal muscle processed for transmission electron microscopy (**A-C**). A higher magnification shows the typical arrangement of 6 actin filaments around each myosin filament (**C**). Scale bars: A, 100 nm; B, C, 50 nm.

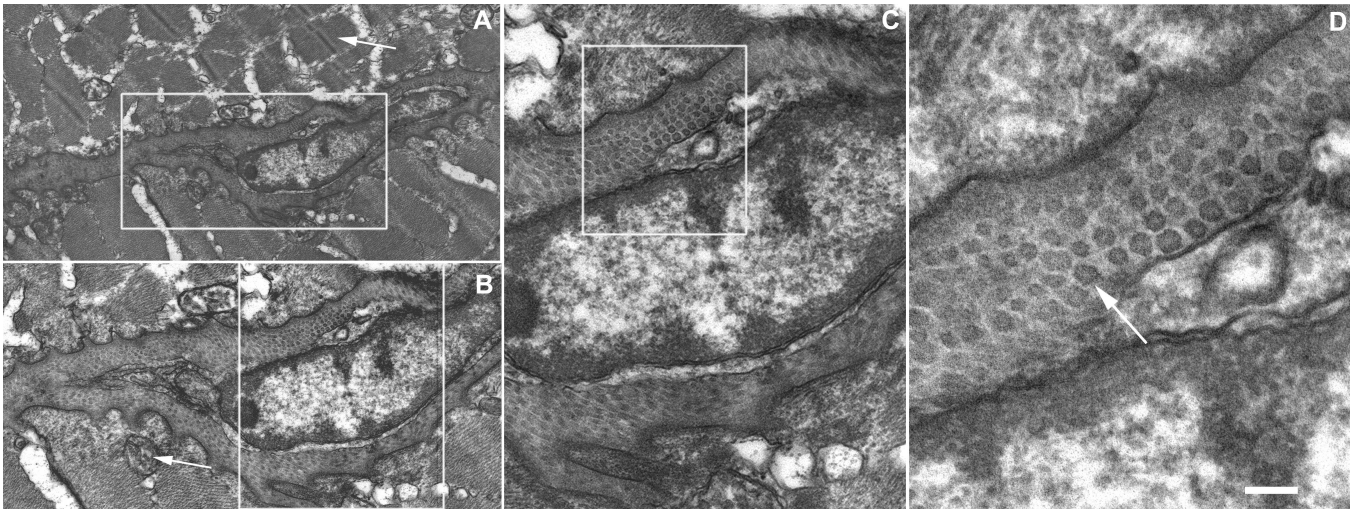

Fig. 7. Ultrastructure of myosepta in the adult zebrafish skeletal muscle. Electron micrographs of a myoseptal region show a centrally located fibroblastic cell (within the white boxes) in the extracellular space between two striated myomere regions (**A**, arrow points to a sarcomere). Many mitochondria were found in close proximity of myofibrils (**B**, arrow). Successive enlargements of specific areas of images (marked with white boxes) show bundles of collagen fibers (**D**, arrow) around the fibroblastic cell. Scale bar: 100 nm.

We used indirect immunofluorescence microscopy of frozen adult skeletal muscle sections to study the muscle cytoskeletal architecture and location of the myofibrillar proteins desmin, alpha-actinin, myosin, titin, troponin, tropomyosin and nebulin, the adhesion proteins vinculin and paxillin, and the extracellular matrix proteins laminin and fibronectin. Using digital image processing and analysis of stains for sarcomeric proteins, we obtained measurements of the sarcomere length that varied from 1.7-2.0 μm. Our measurements are in accordance with the early findings of Waterman (1969). Variations in sarcomere length were attributed to differences in the plane of section relative to the cell axis and/or to the fixation procedure.

The myofibrillar protein complex is made by thin and thick filament systems (composed of actin and myosin molecules, respectively), the third filament system (composed of titin molecules) and the fourth filament system (composed of nebulin molecules). Intermediate filaments are present both at sarcomeric, as well as in extra-sarcomeric regions. Desmin is an intermediate filament protein that is specifically expressed in muscle tissues. It has been described in almost every distinct muscular cytoskeletal structure (Costa et al., 2004), such as Z-bands, costameres (periodic structures in the membrane that are connected to the Z-lines), and the dystrophin adhesion complex. Desmin was sharply localized at the Z-bands of myofibrils in adult zebrafish skeletal muscle. Particularly important is the absence of desmin at myoseptal adhesion structures in the adult zebrafish muscle, such as has been observed by our group in zebrafish embryos (Costa et al., 2008), and in Xenopus embryos (Cary and Klymkowsky, 1994).

In zebrafish, fast muscles are more internal and comprise most of the fish mass, while slow muscles are restricted to the periphery. To study the distribution of the major thick filament protein, myosin II, we tested three different antibodies against myosin heavy chain in the present work: a rabbit polyclonal anti-skeletal myosin, a mouse monoclonal anti-skeletal myosin fast and a mouse monoclonal anti-skeletal myosin slow. The two first antibodies intensely labeled sarcomeric A-bands, while the anti-myosin slow antibody did not show a positive reaction in adult zebrafish muscle. The anti-myosin slow antibody was generated using human immunogen, while the anti-myosin fast was generated using rabbit immunogen. Besides the fact that slow muscles are less frequent, one possible explanation for the lack of slow myosin reaction is that the human epitope that is recognized by the anti-slow myosin antibody is not present in the zebrafish. Other anti-myosin slow and fast antibodies need to be tested in the adult zebrafish muscle in order to confirm this hypothesis.

The third filament system of muscle, which consists of titin, was also analyzed in mature zebrafish muscle. Titin is the largest vertebrate protein known, and spans entire half-sarcomeres. Several monoclonal antibodies have been generated against different titin epitopes, each recognizing a specific sarcomeric region (Fürst et al., 1988). In the present work, we used an anti-titin antibody against the A-I junction to label the adult zebrafish muscle. Nebulin, another giant modular sarcomeric protein, was also studied in frozen sections of the fish muscle. Nebulin makes up the fourth filament system of myofibrils and interacts with actin, tropomyosin and troponin molecules. All of these proteins were localized in the thin filaments regions of sarcomeres, the I-bands.

The extracellular matrix proteins fibronectin and laminin, and the adhesion proteins vinculin and paxillin were all found concentrated at the myoseptal region of the zebrafish adult skeletal muscle. This staining pattern is consistent with earlier reports that showed labeling of the myosepta of adult zebrafish muscle sections using a monoclonal antibody (MANCHO 15 clone) against dystrophin (Chambers et al., 2001) and an antibody against the dystrophin-associated protein δ-sarcoglycan (Guyon et al., 2005). Dystrophin is a sarcolemmal-associated protein that interacts with a dystrophin-associated glycoprotein complex and is thought to provide a link between the cytoskeleton and the extracellular matrix through diverse protein interactions. Therefore, our results provide evidence that the adult zebrafish myoseptal region concentrates extracellular matrix proteins (fibronectin, laminin and collagen) and intracellular adhesion proteins (vinculin and paxillin), all linked by sarcolemmal proteins such as dystrophin.

Even though collagen fibers were easily seen in the myosepta of adult zebrafish muscle analyzed in transmission electron microscopy, we were not able to localize collagen in the immunofluorescence microscopy experiments. We can speculate that the anti-collagen antibody (a monoclonal against human collagen type IV) used did not react with the zebrafish collagen molecules. Other antibodies against collagen proteins should be tested in the zebrafish muscle in order to better understand its distribution in the septal region in comparison with other extracellular matrix components.

It is important to point out that all the antibodies against sarcomeric, adhesion and extracellular proteins used in the present work were generated using avian and mammals as immunogens, and they all showed a high affinity and specificity for the adult zebrafish skeletal muscle, indicating that these proteins have evolutionarily conserved epitopes.

The ultrastructural observations on the adult zebrafish skeletal muscle confirm the earlier data from Waterman (1969) in relation to the distribution of the sarcoplasmic reticulum in close association with most of the myofibrils and in the measurements of sarcomere length within the range of 1.7-2.0 μm. In contrast, no other description on the myoseptal region of adult zebrafish has been done. We found bundles of collagen fibers and centrally located fibroblastic cells in the extracellular space of the septa between the myotomes of the fish. Some of the extracelluar matrix components we

describe, such as collagen, fibronectin and laminin, could be secreted by the fibroblasts. Further studies are necessary in order to understand the role of these cells in the myoseptum. The septal region itself has necessarily a role in the propagation of force in the adult fish, and is suggested to have a role on myogenesis in zebrafish embryos (Kudo et al., 2004); other roles for the septal region in the adult will also have to be uncovered.

The present report is the first description of the distribution of the main sarcomeric and adhesion proteins in mature zebrafish skeletal muscle using immunofluorescence microscopy. Detailed analysis of the distribution of other cytoskeletal and extracellular components in the adult fish muscle is crucial for future investigations on the mechanisms involved in normal and pathological myogenic differentiation in this vertebrate model.

Acknowledgements. We thank Prof. J. Murray (University of Pennsylvania, USA) for his help. This work was supported by Brazilian grants from the Conselho Nacional de Desenvolvimento Científico e Tecnológico (CNPq), the Fundação Carlos Chagas Filho de Apoio à Pesquisa do Estado do Rio de Janeiro (FAPERJ) and the Programa de Apoio à Núcleos de Excelência (Pronex).

References

Bassett D.I. and Currie P.D. (2003). The zebrafish as a model for muscular dystrophy and congenital myopathy. Hum. Mol. Genet. 2, 265-270.

Cary R.B. and Klymkowsky M.W. (1994). Desmin organization during the differentiation of the dorsal myotome in *Xenopus laevis*. Differentiation 56, 31-38.

Chambers S.P., Dodd A., Overall R., Sirey T., Lam L.T., Morris G.E. and Love D.R. (2001). Dystrophin in adult zebrafish muscle. Biochem. Biophys. Res. Commun. 286, 478-483.

Costa M.L., Escaleira R.C., Cataldo A., Oliveira F. and Mermelstein C.S. (2004). Desmin: molecular interactions and putative functions of the muscle intermediate filament protein. Braz. J. Med. Biol. Res. 37, 1819-1830.

Costa M.L., Escaleira R.C., Jazenko F. and Mermelstein C.S. (2008). Cell adhesion in zebrafish myogenesis: distribution of intermediate filaments, microfilaments, intracellular adhesion structures and extracellular matrix. Cell Motil. Cytoskeleton 65, 801-815.

Fürst D.O., Osborn M., Nave R. and Weber K. (1988). The organization of titin filaments in the half-sarcomere revealed by monoclonal antibodies in immunoelectron microscopy: a map of ten nonrepetitive epitopes starting at the Z line extends close to the M line. J. Cell Biol. 106, 1563-1572.

Guyon J.R., Mosley A.N., Juna S.J., Montanaro F., Steffen L.S., Zhou Y., Nigro V., Zon L.I. and Kunkel L.M. (2005). δ-Sarcoglycan is required for early zebrafish muscle organization. Exp. Cell Res. 304, 105-115.

Jackson K.A., Snyder D.S. and Goodell M.A. (2004). Skeletal muscle fiber-specific green autofluorescence: potential for stem cell engraftment artifacts. Stem Cells 22, 180-187.

Kudo H., Amizuka N., Araki K., Inohaya K. and Kudo A. (2004). Zebrafish periostin is required for the adhesion of muscle fiber bundles to the myoseptum and for the differentiation of muscle fibers. Dev. Biol. 267, 473-487.

van Raamsdonk W., Van't Veer L., Veeken K., Tekronnie T. and de Jager S. (1982). Fiber type differentiation in fish. Mol. Physiol. 2, 31-47.

van Raamsdonk W., Smit-Onel M., Scholten G., Hemrika W. and Robbe B. (1987). Metabolic specialization of spinal neurons and the myotomal muscle in post-hatching stages of the zebrafish, *Brachydanio rerio*. A histochemical study. Z. Mikrosk. Anat. Forsch. 101, 318-330.

Waterman R.E. (1969). Development of the lateral musculature in the teleost, *Brachydanio rerio*: a fine structural study. Am. J. Anat. 125, 457-493.

Westerfield M. (2000). The Zebrafish Book: a guide for the laboratory use of zebrafish (*Danio rerio*), Eugene, University of Oregon Press.

Zon L.I. (1999). Zebrafish: A new model for human disease. Genome Res. 9, 99-100.

Accepted September 15, 2008